Quantum oscillations in mesoscopic rings with many chains

Yan Chen
Solid State Microstructure Laboratory and Department of Physics, Nanjing University, Nanjing 210008, China

Shi-Jie Xiong
China Center of Advanced Science and Technology (World Laboratory), P.O. Box 8730, Beijing 100080, China and Solid State Microstructure Laboratory and Department of Physics, Nanjing University, Nanjing 210008, China

S. N. Evangelou
Department of Physics, University of Ioannina, Ioannina 45 110, Greece
(Received 19 February 1997; revised manuscript received 21 April 1997)

We obtain exact analytical expressions for the electronic transport through a multichain system, also in the presence of magneto- and electrostatic fields. The geometrical structure of the electrodes is found to cause a splitting of the conduction band into many subbands depending on the number and the length of the chains, and the conductance approaches zero when the chain number is sufficiently large due to quantum interference. In the presence of a magnetic field very complicated oscillatory behavior of the conductance is found with a very sensitive dependence on the number of chains and their lengths, in a remarkable distinction from the usual two-chain Aharonov-Bohm (AB) ring. A transverse electric bias is found to cause oscillations of the conductance and by increasing the chain number the widths of the resonance peaks become narrower without a change of the oscillation periodicities. If electric and magnetic fields are simultaneously applied the magnetoconductance oscillation pattern depends sensitively on the bias. The present study may provide useful information for quantum device engineering. [S0163-1829(97)01032-1]

I. INTRODUCTION

Quantum transport through artificially fabricated nanostructures has been extensively studied both experimentally and theoretically during the last years.[1,2] The miniaturization of quantum dots or wires has now reached a stage where devices can be fabricated at sizes smaller than the single-particle electronic coherence length. In such mesoscopic systems the wave function maintains its phase coherence so that the electron can travel coherently through the sample. Access to ''coherent transport'' is granted by the advances made in lithography techniques which have opened a very rich field of theoretical and experimental research concerning quantum wires and quantum dots. Electro-optical experiments in solid-state devices could lead to new switches which use the quantum wave nature of the electron.

Many interesting quantum effects can be also found in coupled nanostructures where the electronic transport is drastically affected by quantum interference phenomena. Moreover, the application of a magnetic field, which is often used to probe the properties of devices, can also induce characteristic changes in the phase coherence of the electronic wave functions[3] which, in turn, give rise to particular interference effects for the electronic transport. In the pioneering work of Aharonov and Bohm[4] such an effect was demonstrated via a thought experiment and it was shown that the conductance of a ring should oscillate as a function of the magnetic flux threaded through it. Among the manifestations of the Aharonov Bohm (AB) effect[5–10] usually are the periodic magnetoresistance oscillations in normal metal rings and in electrostatically defined heterjunction rings. The AB effect is a result of the relative phase shift between the two electron beams enclosing a magnetic flux ϕ, where the magnetic field causes a $2\pi(\phi/\phi_0)$ change of the phase difference between the two arms of the ring. In this system the magnetoresistance oscillations have period ϕ_0, which allows tuning of the phase of a wave packet with destructive and constructive interference in cycles. The AB effect in the presence of magnetostatic flux and electrostatic potential has also been discussed.[11–13] The electrostatic AB effect is due to the different phase shifts caused by the potential difference between the two arms. The combination of the electrostatic and magnetostatic AB effect also exhibits interesting conductance oscillation behavior.[13]

Owing to the great variety of the possible configurations for quantum dots it is of great interest to investigate the change of the interference effect in AB rings when the chain number is greater than 2. In this paper, we study the electronic transport properties of a multichain structure with common leads attached at its ends. We show that it can provide many alternative options to the usual AB effect for tuning quantum interference in the electronic transport. In the considered structure an initial wave splits up into complementary waves $\psi_1 \ldots \psi_N$, where N is the total number of chains involved. These waves propagate independently in every chain and are finally recombined at the outgoing lead. Interference effects among the different waves can be observed from the behavior of the electrical resistance obtained between the two leads. We also show that if the number of chains involved is large enough most of the states are reflected and only a few of them can propagate through the system. This kind of ''blocking'' or ''localization'' of the electron waves via quantum interference due to the geometri-

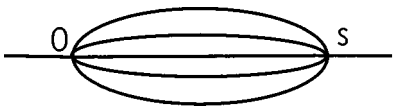

FIG. 1. The considered multichain system with the left and right nodes indicated by 0 and s, respectively. The total number of chains is $N=5$ and the number of sites in the αth chain is N_α, $\alpha=1,2,\ldots,N$ without counting the nodes 0 and s.

cal structure, can occur despite the absence of any disorder in the system.

In the presence of a magnetic field the electron moving around a loop will experience a phase change determined by the flux threaded through the loop. In the multichain system the phase changes are not the same for different paths of propagation so they can lead to particular interference phenomena accompanied by much more complicated conductance oscillations than in the ordinary two-chain AB ring. We find that the pattern of these magnetoquantum oscillations is very sensitive to the number and the length distribution of the chains involved in the structure. Moreover, the oscillation patterns and their periodicities are very sensitive to the partitioning of the flux among the areas enclosed by the paths. The obtained electrostatic conductance oscillations have unchanged periodicities although the resonance peaks become narrower by increasing the chain number. In the presence of both magnetic flux and electrostatic bias a more drastic change of the magnetoconductance oscillation pattern can be seen. At the same time, if the magnetic flux is large enough the electrostatic oscillations of the electron transmission exhibit an abrupt drop from maximum to minimum in every period. It should be pointed out that the results obtained in this paper could be useful towards understanding quantum dots with a special configuration.

The structure of the paper with the exposition of our results is as follows: in Sec. II we describe the studied structure and give analytic expressions for the electronic transport, in Sec. III we demonstrate different kinds of transport induced by special quantum interference effects with and without magnetic flux and transverse electrostatic bias. The obtained results are summarized and discussed in Sec. IV.

II. MODEL AND FORMULA

We consider a ring which consists of many chains with two common leads at their ends threaded by a magnetic field which produces a flux in every loop enclosed by two nearest-neighbor chains. In addition we suppose that the multichain system is embedded in an infinite perfectly conducting chain with a left and a right part serving as the two electrodes. The configuration is shown in Fig. 1 and the transport properties for non-interacting electrons in this system are studied via the tight-binding Hamiltonian

$$H=\sum_{\alpha=1}^{N}\left[V_\alpha\sum_{i=1}^{N_\alpha}c_{\alpha,i}^{\dagger}\,c_{\alpha,i}-t_0\left(c_0^{\dagger}\,c_{\alpha,1}+e^{i\phi_\alpha}c_{\alpha,N_\alpha}^{\dagger}c_s+\sum_{i=1}^{N_\alpha-1}c_{\alpha,i}^{\dagger}\,c_{\alpha,i+1}+\text{H.c.}\right)\right], \tag{1}$$

where $c_{i,\alpha}$ ($c_{i,\alpha}^{\dagger}$) is the annihilation (creation) operator which iannihilates (creates) an electron on the site i of chain α, N_α s the number of sites in the αth chain (excluding the two nodes), N is the total number of chains and the two lead node sites are labeled by 0 and s. The first sum is due to an applied electrostatic bias in the transverse direction so that the potential V_α depends only on the chain index α. The next two terms in Eq. (1) describe hopping of the electrons between the ends of every chain α and the two leads 0 and s and the final term describes hopping between the nearest-neighbor sites in every chain. Moreover, since the chains are connected to each other only at their ends 0 and s we made a convenient choice of the gauge for the vector potential to affect only the phase of the wave functions at the hopping bonds between the right ends of each chain (site $N_\alpha,\alpha=1,2,\ldots,N$) and the right node s. Thus, in the Hamiltonian of Eq. (1) the magnetic field is expressed via the third term in the sum with the phase difference $\phi_\alpha-\phi_{\alpha-1}$ proportional to the flux HW_α, $\alpha=2,3,\ldots,N$, H being the strength of the magnetic field and W_α is the area enclosed by the α and $(\alpha-1)$th chains. The phase of the first chain is chosen to be zero $\phi_1=0$ and the hopping strength for all the bonds $t_0=1$ is the energy unit used throughout the paper.

An experimental realization of the considered chain system is the GaAs quantum wire. This structure has been proposed for an experimental design of AB interferometers by Bandyopadhyay and Porod,[11] since the wires can be made so narrow to carry only one transverse channel. The localization effects in this system can be minimized because of the high mobility of GaAs. Moreover, at low temperatures the relevant length is shorter than the inelastic mean-free path and the structure is essentially ballistic. The carrier density of the GaAs quantum wire is about 10^8 m^{-1} and according to Kane's formula[14] the renormalized coupling constant g is very close to 1. Thus, the one-dimensional electron system may be reasonably treated in the free-electron approximation.[13] If we adopt the above analysis we can neglect the Coulomb interaction and/or inelastic scattering from our discussion.

Our picture of the electronic transport consists of an electron wave incident from the source into the perfect chain, then ramified into the N chains of the structure, experiencing different phase increments, and eventually recombined into one channel at the output lead. Thus, an electronic beam incident from the right should be partially transmitted and partially reflected by the multichain system. In the site representation the coefficients of the wave function at the left and the right parts of the pure chain can be written as

$$a_j=e^{-ikj},\quad \text{for } j\leqslant 0,$$

$$a_j=Ae^{-ik(j-s)}+Re^{ik(j-s)},\quad \text{for } j\geqslant s, \tag{2}$$

where $k=\cos^{-1}(E/2)$ is the wave vector of a wave function with energy E, A is the amplitude of the incident wave, R is the amplitude of the reflected wave, and the wave function is normalized so that the transmitted wave amplitude is unity. The transmission coefficient which measures the transparancy of the system can be subsequently defined as $|t|^2=1/|A|^2$. The wave-function coefficients in the αth chain,

by including the left node 0, can be expressed as a linear combination of the propagating and the reflected plane waves via

$$a_{\alpha,j}=A_\alpha e^{ik_\alpha j}+R_\alpha e^{-ik_\alpha j}, \quad \text{for } 0\leqslant j\leqslant N_\alpha, \tag{3}$$

where $a_{\alpha,j}$ is the coefficient at the jth site of the αth chain and $k_\alpha=\cos^{-1}((E-V_\alpha)/2)$ is the electron wave vector of the α chain in the electrostatic potential V_α.

The coefficient at the left lead node $j=0$ from Eqs. (2) and (3) gives the relation

$$A_\alpha+R_\alpha=1. \tag{4}$$

Similarly, we can calculate the coefficient at the right node $j=s$, by including the flux-induced phase shift term, and a comparison with Eq. (2) gives a second relation

$$(A_\alpha e^{ik_\alpha(N_\alpha+1)}+R_\alpha e^{-ik_\alpha(N_\alpha+1)})e^{-i\phi_\alpha}=A+R. \tag{5}$$

Therefore, from the two Eqs. (4) and (5) we can express the wave-function coefficient of Eq. (3) for all chains α via

$$A_\alpha=-\frac{e^{-ik_\alpha(N_\alpha+1)}-(A+R)e^{i\phi_\alpha}}{2i\ \sin(k_\alpha(N_\alpha+1))}, \tag{6}$$

$$R_\alpha=\frac{e^{ik_\alpha(N_\alpha+1)}-(A+R)e^{i\phi_\alpha}}{2i\ \sin(k_\alpha(N_\alpha+1))}, \tag{7}$$

in terms of A and R.

On the other hand, from the Schrödinger difference equations at the two lead nodes 0 and s we obtain

$$E=e^{ik}+\sum_\alpha\ (A_\alpha e^{ik_\alpha}+R_\alpha e^{-ik_\alpha}), \tag{8}$$

$$E(A+R)=Ae^{-ik}+Re^{ik}+\sum_\alpha\ e^{-i\phi_\alpha}(A_\alpha e^{ik_\alpha N_\alpha} + R_\alpha e^{-ik_\alpha N_\alpha}), \tag{9}$$

and by a substitution of Eqs. (6), (7) into Eqs. (8), (9) eventually obtain two equations for A and R. Finally, the transmission coefficient can be calculated from their solution which gives

$$|t|^2=\frac{4|f_0|^2\sin^2k}{|(c_0-e^{-ik})^2-|f_0|^2|^2}, \tag{10}$$

where

$$f_0=\sum_\alpha\ \frac{e^{i\phi_1}e^{i(\phi_\alpha-\phi_1)}\sin k_\alpha}{\sin(k_\alpha(N_\alpha+1))},$$

and

$$c_0=\sum_\alpha\ \frac{\sin k_\alpha N_\alpha}{\sin(k_\alpha(N_\alpha+1))},$$

for arbitrary chain lengths $N_\alpha, \alpha=1,2,\ldots,N$.

Equation (10) is the most important result of this paper, which presents the general analytical expression for the transmission coefficient in a multichain ring. This expression can be further simplified for special geometries, for example, if the chain lengths are equal to $N_1=N_2=\ldots=N_N\equiv L$, and the two nearest-neighbor chains enclose a fixed area $\phi=\phi_\alpha-\phi_{\alpha-1}$ in the absence of electrostatic potential

$$f_0=\frac{e^{i(N-1)\phi/2}\sin(N\phi/2)\sin k}{\sin(\phi/2)\sin(k(L+1))}, \tag{11}$$

$$c_0=\frac{N\ \sin kL}{\sin(k(L+1))}, \tag{12}$$

and a simpler exact expression for the transmission coefficient $|t(E)|^2$ can be obtained. It can be seen from Eq. (10) that the magnetic-field dependence is solely due to $|f_0|$ so that if the factors $1/W_2$, $1/(W_2+W_3),\ldots,1/\Sigma_{\alpha=2}^N W_\alpha$ have common multiples the oscillations of $|t(E)|^2$ as a function of a magnetic field have a period of $\nu\phi_0$, where ν is the smallest common multiple with ϕ_0 being the flux quantum. The electronic conductance can be also directly computed from the transmission coefficient via the Landauer formula[15]

$$\sigma(E)=\frac{|t(E)|^2}{1-|t(E)|^2}, \tag{13}$$

at the Fermi energy E.

III. QUANTUM OSCILLATIONS FOR VARIOUS MULTICHAIN CONFIGURATIONS

In this section we show our results associated with quantum interference effects in multichain systems by application of Eq. (10). Our purpose is to illustrate the electronic wave transport in the geometric multichain ring structure, also in the presence of external fields.

A. Equal chain system without fields

In the absence of a magnetic field the replacement $\phi=0$ for f_0, c_0 is made in Eqs. (11), (12). The obtained results in this case correspond to a similar model of a total number of N thin wires joined together at their two ends as it was introduced by Wang *et al.*[16] in their study of electronic transport through a quantum cavity. These authors have predicted that the total electron transmission can be simply expressed as a coherent sum of the transmission coefficients obtained from every chain. Our results can give even more complicated transmission behavior due to the geometrical structure of the electrodes.

In Fig. 2 we plot the transmission coefficient versus the electronic energy for such a multichain system made of equal chains. The pattern shown exhibits an interesting bridge-arc shape whose curvature becomes larger and the blank region below the arc smaller if the chain number increases, with some states still having high values of the transmission coefficient. Thus, if the chain number is large enough most of the states are reflected and only very few states can propagate through the system. It must be emphasized that the blocking of the electron propagation at most energies is merely caused by quantum interference due to the geometrical structure involved. It seems, however, a puzzle why such a rather symmetric geometry can give rise to a very complicated behavior of the outgoing wave. This is probably due to the fact that the translation symmetry is broken at the two

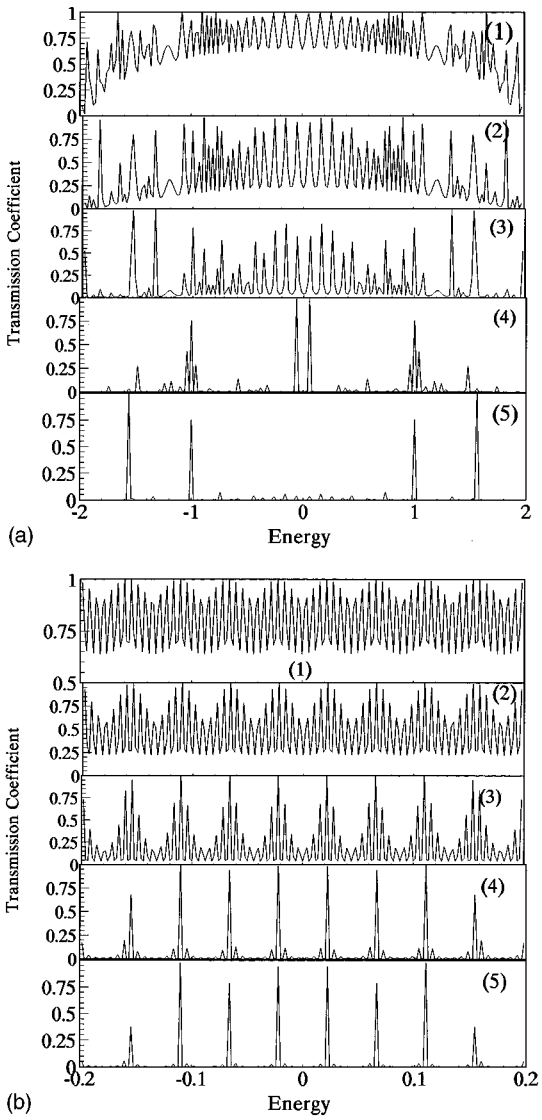

FIG. 2. The transmission coefficient as a function of the electronic energy for a N-chain system of equal chain lengths (a) $L=N_\alpha=100$, $\alpha=1,2,\ldots,N$ and (b) $L=1000$. The chain numbers involved in each case are (1) $N=2$, (2) $N=4$, (3) $N=10$, (4) $N=40$, and (5) $N=80$.

contacts, which leads to partial destructive interference of the electron waves. Wang *et al.*[16] have also observed a partial blocking of electron waves by varying the electronic wavelength in the propagation regime of a quantum-wave filter consisting of field-induced nanoscale cavities and 1D wires. Our results could account for the reported experimental behavior.

We have also investigated the relationship between the obtained features of the conducting spectrum and the chain number for an equal chain multichain system. In Fig. 3 the conduction band as a function of the number of chains is illustrated and we observe that by increasing the chain number the transmission pattern becomes more and more sparse and the conduction band splits into several subbands. If the number of chains becomes large enough we find that most of the states cannot propagate through the system, becoming ''blocked'' or ''localized.'' Thus, the conduction band becomes discrete due to quantum interference in the absence of

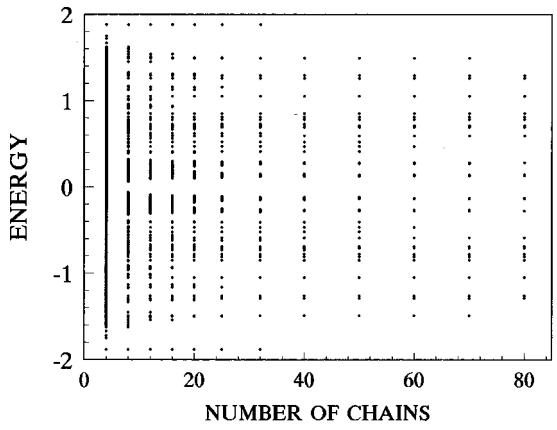

FIG. 3. The conduction band vs the chain number N for a multichain system with chain lengths $N_\alpha=5000$, $\alpha=1,2,\ldots,N$. A conduction band is defined as being nonzero at the energy values where the corresponding transmission coefficient is higher than 0.1.

disorder and/or interchain couplings, except at the two end node connections. A relation between the conductance and the chain number can be extracted from Fig. 4, where a monotonic drop of the conductance is seen when the number of chains is increased. This is another indication of the trend shown by the system to become more ''insulating'' for large chain numbers.

B. Magnetoconductance oscillations

In Fig. 5(a) we show the characteristics of the transmission coefficient obtained in the absence of a magnetic field, such as the bridge-arc shape already seen in Fig. 2(a), in order to compare with the cases with an applied magnetic field [Figs. 5(b), 5(c), and 5(d)]. We find a remarkable change of the transmission in the latter case when the areas between neighboring chains enclose equal magnetic fluxes. In Figs. 5(b), 5(c), and 5(d) the arc structure is no longer present and the transmission becomes more and more sparse due to the higher magnetic flux through the system.

In Fig. 6 we present the magnetic-field dependence of the transmission coefficient for equal chains with the same nearest-neighbor path areas. In this case the curves show periodic quantum-magnetic oscillations governed by the field

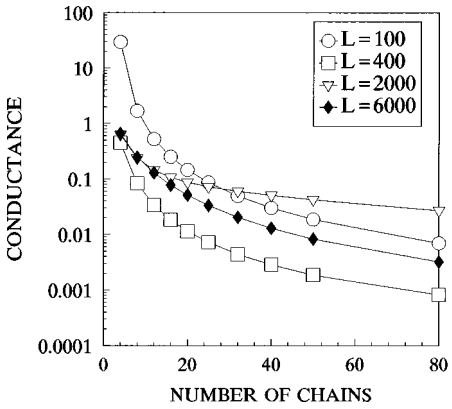

FIG. 4. The conductance $\sigma(E)$ as a function of the number of chains N for a system with equal chains of length $L=N_\alpha$, $\alpha=1,2,\ldots,N$, at a Fermi energy $E=1.0$, in the absence of a magnetic field.

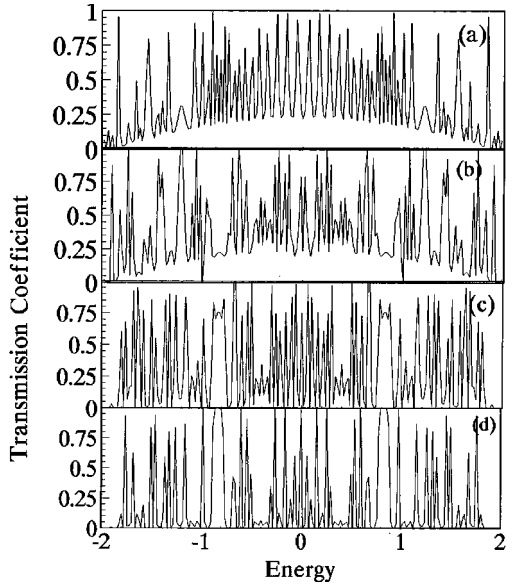

FIG. 5. A comparison of the transmission coefficient with and without a magnetic field. The structure consists of $N=4$ chains of lengths $L=N_\alpha=2000$, $\alpha=1,2,3,4$ and the magnetic flux threaded in the system is (a) 0, (b) 0.1, (c) 0.5, and (d) 2.0.

dependence which enters f_0 via Eqs. (11) and (12), finally leading to $(N-1)\phi_0$. These findings share many similarities with the optical multislit interference patterns[5,6] with main common features the $N-1$ minima and the $N-2$ subsidiary maxima between every two consecutive principal maxima. However, the obtained electronic transmission is more complicated when compared to the analogous optical case due to the complexity of the denominator in our expression for $|t(E)|^2$. Moreover, from Fig. 6 we can observe many points of zero transmission which imply a magnetic-field-induced destructive interference effect.

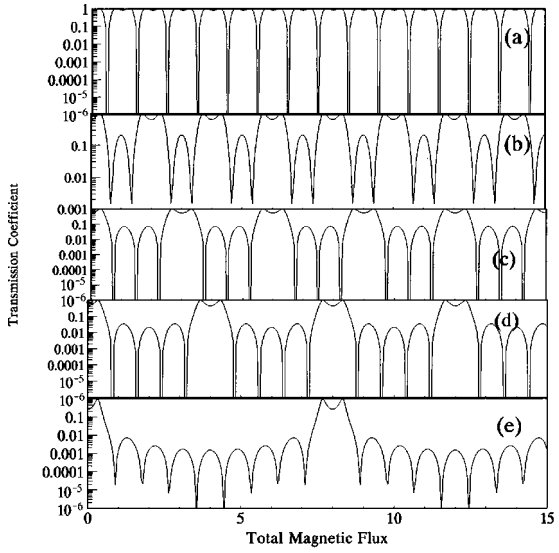

FIG. 6. The electronic transmission vs the magnetic flux for a multichain system with equal chain lengths $L=N_\alpha=2000$, $\alpha=1,2,\ldots,N$ and fixed electron energy $E=1.1$. The unit of the magnetic flux is the flux quantum $\phi_0=1$ and the chain numbers are (a) $N=2$, (b) $N=3$, (c) $N=4$, (d) $N=5$, and (e) $N=9$.

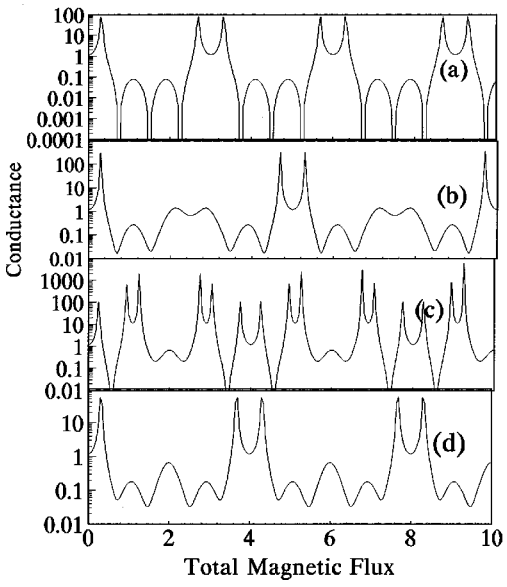

FIG. 7. The electronic conductance vs the magnetic flux for a multichain system $(N=4)$ with equal chain lengths $L=N_\alpha=2000$, $\alpha=1,2,3,4$ and electron energy fixed at $E=1.1$, with the magnetic flux quantum $\phi_0=1$. (a) $\phi_2-\phi_1=\phi_3-\phi_2=\phi_4-\phi_3$, (b) $\phi_2-\phi_1=\phi_3-\phi_2=\frac{1}{2}(\phi_4-\phi_3)$, (c) $\phi_2-\phi_1=3$ $\phi_3-\phi_2$ and $\phi_4-\phi_3=0$, (d) $\phi_2-\phi_1=\phi_3-\phi_2=2(\phi_4-\phi_3)$.

Our results for a system with equal chains but nonequal areas enclosed by every two nearest-neighbor paths are shown in Figs. 7 and 8. It can be seen that the interference pattern and the magnetoscillation periods vary, depending on the distribution of the magnetic flux between the closed paths. In Fig. 7 we show the electronic conductance versus the magnetic flux for a four-chain system made of equal chains with magnetic flux periods (a) $3\phi_0$, (b) $5\phi_0$, (c) $4\phi_0$, and (d) $4\phi_0$. One can easily deduce the relation between the oscillation period and the distribution of the mag-

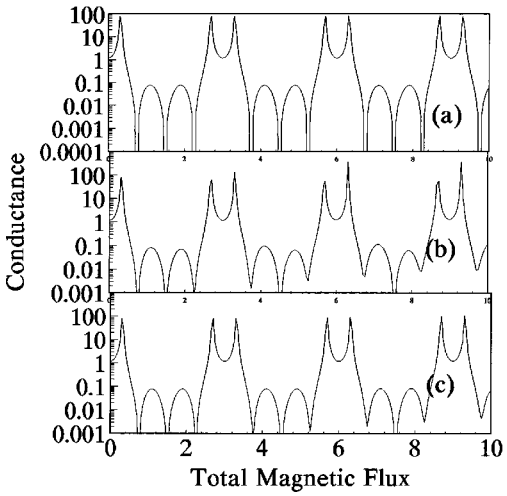

FIG. 8. The electronic conductance vs the magnetic flux for a multichain system $(N=4)$ with equal chain lengths $L=N_\alpha=2000$, $\alpha=1,2,3,4$ and electron energy fixed at $E=1.1$, with the magnetic flux quantum $\phi_0=1$: (a) $\phi_2-\phi_1=\phi_3-\phi_2=\phi_4-\phi_3$, (b) $0.99(\phi_2-\phi_1)=\phi_3-\phi_2=1.01(\phi_4-\phi_3)$, (c) $0.98(\phi_2-\phi_1)=\phi_3-\phi_2=1.01(\phi_4-\phi_3)$.

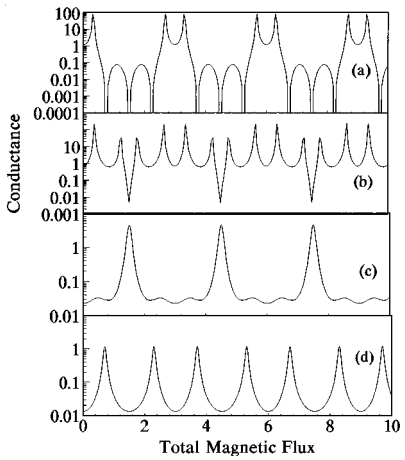

FIG. 9. The electronic conductance vs the magnetic flux for a multichain system ($N=4$) with almost equal chain lengths N_α, $\alpha=1,2,3,4$ and electron energy fixed at $E=1.1$ with the magnetic flux quantum $\phi_0=1$: (a) the chain lengths are (a) $N_\alpha=2000$, $\alpha=1,2,3,4$, (b) $N_1=2000$, $N_2=2002$, $N_3=2004$, $N_4=2006$, (c) $N_1=2000$, $N_2=2010$, $N_3=2020$, $N_4=2030$, (d) $N_1=2000$, $N_2=2100$, $N_3=2200$, $N_4=2300$.

netic fluxes by noticing that the phase shift for every chain must be an integer times 2π. If the magnetic flux distribution has small deviations the mageto-oscillation pattern and its period changes abruptly, as shown in Fig. 8. Without any deviation, the spectrum has a strict period of 3π and destructive interference occurs twice during this period. Introducing small deviations, the spectrum has no longer strict periodicity and the interference pattern changes aperiodically.

In Fig. 9 we present results for a system of both different chain lengths and nonequal areas enclosed by two nearest-neighbor paths. From the realizations of Eq. (10) we find that the conductance changes when the chain length varies because of variations in both the numerator and the denominator of Eq. (10). For a certain length distribution we observe a quasiperiodic pattern close to about $1.5\phi_0$, but its real period is $3\phi_0$ as in Fig. 9(d). Thus, we may conclude that even a small variation of the chain lengths can cause abrupt changes in the conductance oscillation patterns. It is, perhaps, worth mentioning that the sensitivity found could provide an opportunity for applications of the studied multichain structure to electronic device engineering.

C. Electro- and magnetoconductance oscillations

In this subsection, we investigate the influence of an additional electric bias on the conductance of the system. In Fig. 10, we show the characteristics of the transmission vs the electrostatic potential for a system with different chain numbers. We observe periodic oscillatory behavior and by increasing the chain number the period of the oscillations remains unchanged but the widths of the resonance peaks become narrower with the distance between minimum and maximum decreased in each period. If the chain number reaches 80 the maximum to minimum value ratio is nearly 500. These results are similar to those obtained in the study of serially connected mesoscopic rings.[13] The corresponding magetoconductance oscillation pattern in the presence of

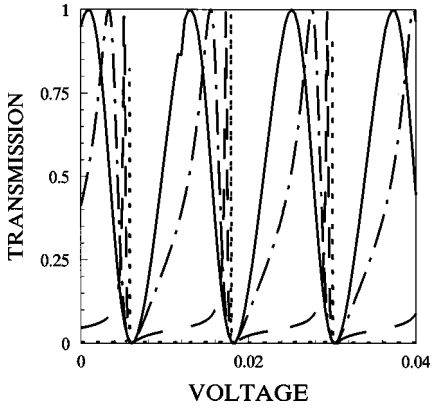

FIG. 10. The transmission coefficients vs the electrostatic potential for systems with various chain numbers, equal chain lengths $L=N_\alpha=1000$, $\alpha=1,2,3,4$ and an electric bias $V=0.5$. The chain numbers are (a) $N=2$ for the solid line, (b) $N=6$ for the dotted-dashed line, (c) $N=20$ for the dashed line, and (d) $N=80$ for the dotted line.

electrostatic bias can be seen in Fig. 11 where a drastic effect of the magnitude of the bias to the oscillation pattern is shown. If the voltage is increased the number of the secondary maxima in every oscillation period first decreases and then recovers the zero-bias value. This implies an oscillatory effect of the bias on the magnetoquantum oscillations.

Figure 12 shows electroconductance oscillations under different values of the magnetic flux. It can be observed that the periodicity is not changed by variations of the magnetic flux. It is seen, however, that by increasing the magnetic flux the transition from maximum to minimum in each period of oscillation is sharpened and the width of resonance regions becomes very narrow. It is interesting to point out that for zero magnetic flux there is only a single peak in every period but by applying a nonzero flux two peaks appear with one of them extremely sharp.

IV. DISCUSSION

Quantum interference plays a central role in the quantum physics of mesoscopic systems. We have shown that for a

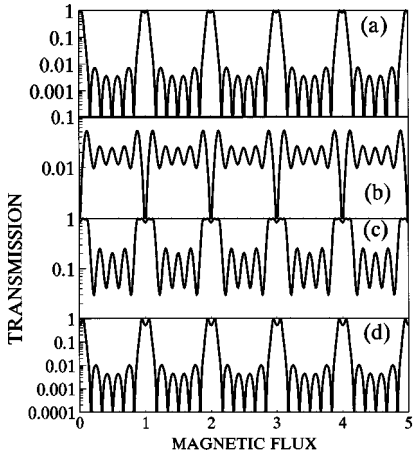

FIG. 11. The electronic transmission vs the magnetic flux for a multichain system ($N=6$) with equal chain lengths $L=N_\alpha=1000$, $\alpha=1,2,\ldots,N$: The electrostatic bias is (a) $V=0$, (b) $V=0.004$, (c) $V=0.008$, and (d) $V=0.012$.

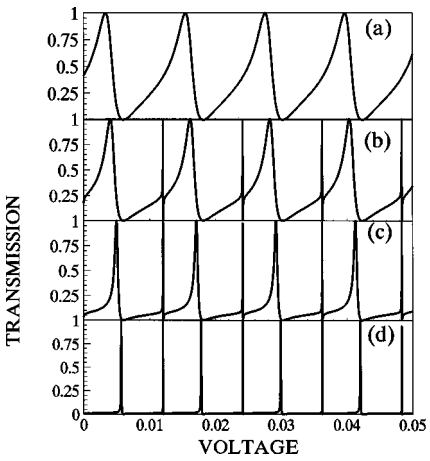

FIG. 12. The electronic transmission vs the electric bias with the rest of parameters the same as in Fig. 11. The magnetic flux is (a) $\phi=0$, (b) $\phi=0.01$, (c) $\phi=0.02$, and (d) $\phi=0.04$.

multichain system an incident wave splits into several chain beams at the entrance and recombines at the exit. Thus, the conduction band becomes discrete and the electronic transport properties are drastically modified by a ''localization'' effect, despite the absence of any disorder. Moreover, in the presence of a magnetic flux we obtain magneto-oscillations, which are much more complicated than these known in the usual AB rings. In the AB effect a magnetic field is threaded through the center of a ring so that the electrons passing via each of the two chains experience different phase shifts. If we vary the magnetic field one can modulate the phase and produce conductance oscillations in the wave transport from one terminal to the other. We show that the transmission as a function of an electric bias also exhibits a miniband structure, similar to that obtained for serially connected AB rings.[13] However, the origin for the similar behavior in the two cases is different, since in Ref. 13 the N connected rings correspond to N tunneling barriers in one-dimensional superlattices which give $N-1$ resonance peaks in the transmission curves. In our ring structure it is the presence of many chains which provides channels with different phase shifts due to the bias, finally inducing destructive or constructive interferences. Thus, the physical origin of the miniband structure in our case is solely due to the considered multichain ring geometry.

The magnetic-field dependence of the electrical conductance also shows an oscillating behavior different from the AB ring effect, since the multichain system exhibits more complicated interference phenomena determined by the phase shifts in the various propagation paths. Each phase shift is caused by both the electronic momentum and the magnetic flux, so that momentum variations and changes in the chain lengths as well as variations in the distribution of the magnetic fluxes can modify the interference pattern. Electron wave propagation through our multichain system pierced by a magnetic field has also an interesting analogy with optical interference phenomena by many slits. In both phenomena $N-2$ subsidiary maxima and $N-1$ minima between two consecutive principal maxima occur. Of course, between each pair of minima a subsidiary maximum exists,[17] as confirmed by our numerical calculations. In the presence of a transverse electric bias the conductance also oscillates as a function of the bias. If the chain number increases the periodity of the oscillation does not change but the widths of the resonance peaks become narrower. Furthermore, in the presence of both electric and magnetic fields the magneto-conductance oscillation pattern is very sensitive on the bias. Questions refering to more appropriate conductance formulas can be found in Ref. 18 and the AB oscillations in a ring with a quantum dot inserted in one of its arms is studied in Ref. 19.

It must be pointed out that our results are also relevant for the case of Andreev scattering[20] which occurs in normal-superconductor interfaces. It turns out that if the right-hand side periodic chain attached to the considered dot structure is replaced by a clean superconducting wire the obtained results for the transmission coefficient of the normal-dot-normal geometry can be used for finding the transmission through the normal-dot-superconductor system. This is achieved via Beenaker's formula[21] for the conductance $G=(2e^2/h)2|t|^4/(2-|t|^2)^2$, which is expressed via the transmission of the nonsuperconducting part only. If we use the obtained $|t|^2$ from Eq. (10) an extra doubling of periodicity is expected for the dot-superconductor interface.

In summary, we have systematically studied the electronic properties of a multichain system connected at its two ends. A recursion method was employed and an exact analytic expression for the electronic conductance was presented. Many interesting features of the transmission coefficient, the magneto- and electroconductance were shown for various configurations: (1) The geometrical structure of the electrodes is found to cause a discreteness of the conduction band, which eventually affects remarkably the transport properties leading to a kind of ''localization'' in the absence of disorder. (2) We find various magneto-oscillation periodicities and interference patterns by varying the distribution of the relative magnetic flux through the structure and abrupt changes of the conductance versus the magnetic flux if the length distribution of the system is modulated, which is useful to distingush even slight chain length variations. (3) The studied system can be also used to probe the distribution of the magnetic field since the obtained interference patterns are very sensitive to the distribution of the magnetic flux among neighboring closed paths. (4) The small ratio of the resonance peak widths to the period of the oscillation in the plots of conductance vs the electric bias for large enough chain numbers may be useful for quantum device engineering.

ACKNOWLEDGMENTS

This work was supported by the National Natural Science Foundation of China, a $\Pi.EN.E.\Delta.$ grant of the Greek Secretariat of Science and Technology, and HCM, TMR programs of the E.U. We also like to thank Professor Colin Lambert for pointing out the relevance of our results for normal-superconducting interfaces.

[1] For reviews, see *Mesoscopic Phenomena in Solids*, edited by B.L. Altshuler, P.A. Lee, and R.A. Webb (North-Holland, New York, 1991).
[2] See, also, *Transport Phenomena in Mescoscopic Systems*, edited by H. Fukuyama and T. Ando (Springer-Verlag, Berlin, 1992).
[3] N. Byers and C. N. Yang, Phys. Rev. Lett. **7**, 46 (1961).
[4] Y. Aharanov and D. Bohm, Phys. Rev. **115**, 485 (1959).
[5] M. Peshkin and A. Tonomura, *The Aharonov-Bohm Effect* (Springer-Verlag, Berlin, 1990).
[6] A. Tonomura, Adv. Phys. **41**, 59 (1992).
[7] R. A. Webb, S. Washburn, C. P. Umbach, and R. B. Laibowitz, Phys. Rev. Lett. **54**, 2696 (1985).
[8] I. V. Krive and A. S. Roshansky, Int. J. Mod. Phys. B **6**, 1255 (1985).
[9] G. Matteucci and G. Pozzi, Phys. Rev. Lett. **54**, 2469 (1985).
[10] M. Buttiker, Y. Imry, and R. Landauer, Phys. Lett. **96A**, 365 (1983); M. Buttiker, Y. Imry, and M. Ya. Azbel, Phys. Rev. A **30**, 1982 (1984).
[11] S. Bandyopadhyay and W. Porod, Superlattices Microstruct. **5**, 239 (1989).
[12] M. Cahay, S. Bandyopadhyay, and H. L. Grubin, Phys. Rev. B **39**, 12 989 (1989).
[13] D. Takai and K. Ohta, Phys. Rev. B **48**, 1537 (1993); **50**, 2685 (1994); **50**, 18 250 (1994); **51**, 11 132 (1995).
[14] C. L. Kane and M. P. A. Fisher, Phys. Rev. Lett. **68**, 1220 (1992).
[15] R. Landauer, IBM J. Res. Dev. **1**, 223 (1957); Philos. Mag. **21**, 863 (1970).
[16] Y. Wang, W. Y. Deng, and S. Y. Chou, Superlattices Microstruct. **17**, 193 (1995).
[17] See, for example, E. Hecht and A. Zajac, *Optics* (Addison Wesley, Reading, MA 1974).
[18] M. Buttiker, Phys. Rev. Lett. **57**, 1761 (1986).
[19] A. Levy Yeyati and M. Buttiker, Phys. Rev. B **52**, R14 360 (1995).
[20] A. F. Andreev, Sov. Phys. JETP **19**, 1228 (1964).
[21] C. W. J. Beenakker, Phys. Rev. B **46**, 12 841 (1992).